

Numerical Simulation of Multi-phase Flow in Porous Media on Parallel Computers

Hui Liu*, Lihua Shen, Kun Wang, Bo Yang, Zhangxin Chen
Department of Chemical and Petroleum Engineering
University of Calgary, 2500 University Drive NW, Calgary, AB, Canada

Abstract

A parallel reservoir simulator has been developed, which is designed for large-scale black oil simulations. It handles three phases, including water, oil and gas, and three components, including water, oil and gas. This simulator can calculate traditional reservoir models and naturally fractured models. Various well operations are supported, such as water flooding, gas flooding and polymer flooding. The operation constraints can be fixed bottom-hole pressure, a fixed fluid rate, and combinations of them. The simulator is based on our in-house platform, which provides grids, cell-centred data, linear solvers, preconditioners and well modeling. The simulator and the platform use MPI for communications among computation nodes. Our simulator is capable of simulating giant reservoir models with hundreds of millions of grid cells. Numerical simulations show that our simulator matches with commercial simulators and it has excellent scalability.

Keywords: Reservoir Simulation, Black oil, Oil-water, Parallel Computing

1 INTRODUCTION

Reservoir simulations are powerful tools for petroleum engineers. Simulators can be used to model oil, gas and water flow underground and interactions between reservoirs and wells, which can predict well performance, such as oil rates, gas rates, water rates and bottom hole pressure. These tools are employed to validate and optimize well operations. Inputs of reservoir simulators include properties of fluids and reservoir rock. Geological models of reservoirs can be obtained from seismic imaging. Usually they are complex and highly heterogeneous, which introduce numerical difficulties for reservoir simulators. When a reservoir model is large enough, a typical simulator may take days or even longer to complete one simulation study case, especially in thermal simulations. Effective numerical methods, linear solvers, and fast computing techniques need be studied.

*Authors to whom Correspondence may be addressed. Email addresses: hui.jw.liu@gmail.com

Reservoir simulation has been a popular research topic for decades. Various reservoir models and well treatments as well as their numerical methods^[12] and fast computer techniques have been developed^[6,18,19]. Chen et al. studied finite element methods and finite difference methods for the black oil, compositional and thermal models^[12]. Newton methods, linear solvers and preconditioners were also studied^[12]. Kaarstad et al.^[3] implemented a parallel two-phase oil-water simulator. Rutledge et al.^[1] implemented a compositional simulator, which was designed for parallel computers. The simulator used the IMPES (implicit pressure-explicit saturation) method and only pressure was solved for. Shiralkar and his collaborators^[2] developed a portable parallel reservoir simulator, which could run on a variety of parallel systems. Killough et al.^[4] studied locally refinement techniques, which could improve accuracy and reduce calculations compared with global grid refinement. The technique is useful to complex reservoir models, such as in-situ combustion. Dogru and his group^[5] developed parallel simulators using structured and unstructured grids, which could handle faults, pinchouts, complex wells, polymer flooding in non-fractured and fractured reservoirs. Their parallel simulator was highly efficient and scalable, and it could compute giant reservoir models with billions of grid cells. Zhang et al. developed a general-purpose parallel platform for large-scale scientific applications. The platform was designed for adaptive finite element and adaptive finite volume methods^[6,7], and it used tetrahedral grids. The newest-vertex based bisection refinement method, various linear solvers, preconditioners and eigenvalue solvers were provided. The package has been applied to black oil simulations using discontinuous Galerkin methods^[16]. Chen and his group developed a parallel platform to support the study of large-scale reservoir simulations and this platform was implemented to support black oil, compositional, thermal, and polymer flooding models^[18,21,29]. Guan and his collaborators implemented a parallel simulator, which could compute black oil model and compositional model^[19]. Massive reservoir models with hundreds of millions of grid cells were reported using 10,000 MPIs^[19]. Wheeler has developed a parallel black oil simulator^[20] and she studied numerical methods, linear solvers, and preconditioner techniques. It is well-known that solution of linear systems from black oil simulations occupies most of running time. Many preconditioning methods have been proposed and applied to reservoir simulations, such as constrained pressure residual (CPR) methods^[8,9], multi-stage methods^[10], multiple level preconditioners^[15], fast auxiliary space preconditioners (FASP)^[11], and a family of parallel CPR-like methods^[13].

A black oil simulator has been implemented, which handles several different models, such as the standard three-phase black oil model, two-phase oil-water model, and dual-porosity and dual permeability model in naturally fractured reservoirs. The implementation details are introduced in this paper, including models, numerical methods, and parallel implementations. Numerical experiments show that our simulator can match commercial simulators and it has excellent scalability. Our simulator can compute large-scale reservoir simulation problems with hundreds of millions of grid cells.

2 RESERVOIR SIMULATION MODELS

We assume the fluid in black oil model satisfies Darcy’s law, which establishes a relationship among flow rate, reservoir properties, fluid properties and phase pressure differences, and it is written as:

$$Q = -\frac{\kappa A \Delta p}{\mu L}, \tag{1}$$

where, κ is permeability of rock (or reservoir), A is cross-section area in some direction, Δp is pressure difference, μ is viscosity of the fluid, and L is length of a porous media in the direction. Its differential

form is written as:

$$q = \frac{Q}{A} = -\frac{\kappa}{\mu} \nabla p. \quad (2)$$

2.1 Black Oil Model

The black oil model is isothermal, and it has three components (water, oil and gas) and three phases (water, oil and gas). The gas component can exist in oil phase (solution gas) and gas phase (free gas). The water component exists only in water phase and the oil component exists in oil phase only.

By applying Darcy's law, three mass conservation equations for three components in non-fractured reservoirs are written as:

$$\begin{cases} \frac{\partial}{\partial t}(\phi s_o \rho_o^o) & = \nabla \cdot \left(\frac{KK_{ro}}{\mu_o} \rho_o^o \nabla \Phi_o \right) + q_o, \\ \frac{\partial}{\partial t}(\phi s_w \rho_w) & = \nabla \cdot \left(\frac{KK_{rw}}{\mu_w} \rho_w \nabla \Phi_w \right) + q_w, \\ \frac{\partial(\phi \rho_o^s s_o + \phi \rho_g s_g)}{\partial t} & = \nabla \cdot \left(\frac{KK_{ro}}{\mu_o} \rho_o^s \nabla \Phi_o \right) + q_o^g \\ & + \nabla \cdot \left(\frac{KK_{rg}}{\mu_g} \rho_g \nabla \Phi_g \right) + q_g, \end{cases} \quad (3)$$

where, any phase α ($\alpha = o, w, g$), Φ_α is its potential, ϕ and K are porosity and permeability, and s_α , μ_α , ρ_α , ρ_α^o , $K_{r\alpha}$ and q_α are phase saturation, phase viscosity, phase pressure, phase density, relative permeability and well rate, respectively. ρ_o^o and ρ_o^s are density of oil component in oil phase and density of solution gas in oil phase. They properties have the following constraints:

$$\begin{cases} \Phi_\alpha = p_\alpha + \rho_\alpha Gz, \\ s_o + s_w + s_g = 1, \\ p_w = p_o - p_{cow}(s_w), \\ p_g = p_o + p_{cog}(s_g), \end{cases}$$

where G is the gravitational constant and z is the reservoir depth. In this paper, a no-flow condition is applied as the boundary condition. The relative permeabilities of water phase, gas phase and oil phase, K_{rw} , K_{ro} and K_{rg} are functions of water saturation and gas saturation,

$$\begin{cases} K_{rw} = K_{rw}(S_w), \\ K_{rg} = K_{rg}(S_g), \\ K_{ro} = K_{ro}(S_w, S_g), \end{cases}$$

where K_{ro} is calculated by using the Stone II formula. In our simulator, K_{rw} and K_{ro} are input parameters. The capillary pressures are also input parameters, which are functions of water and gas saturations. Usually oil phase pressure, water saturation, gas saturation (or bubble point pressure) are chosen as unknowns.

For fractured reservoirs, each grid cell is divided into matrices and fracture, and each matrix and fracture have its own pressure, saturation, and conservation laws. The commonly used models are dual porosity model, dual permeability model and MINC (multiple interacting continuum) model. The mass conservation laws are similar to non-fractured reservoirs except that transfer terms should be defined among matrices and fractures.

2.2 Two-Phase Flow Model

The two-phase model ignores gas phase and can be read as a simplified model of the standard black oil model,^[12]:

$$\begin{cases} \frac{\partial}{\partial t}(\phi s_o \rho_o) = \nabla \cdot \left(\frac{KK_{ro}}{\mu_o} \rho_o \nabla \Phi_o \right) + q_o \\ \frac{\partial}{\partial t}(\phi s_w \rho_w) = \nabla \cdot \left(\frac{KK_{rw}}{\mu_w} \rho_w \nabla \Phi_w \right) + q_w. \end{cases} \quad (4)$$

The variables are the same as black oil model and they are the following constraints,

$$\begin{cases} \Phi_\alpha = p_\alpha + \rho_\alpha Gz, \\ s_o + s_w = 1, \\ p_w = p_o - p_{cow}(s_w), \end{cases}$$

and again, G is the gravitational constant and z is the reservoir depth. In our simulator, oil phase pressure and water saturation are chosen as unknowns.

2.3 Well Management

The source-sink model and Peaceman method^[17] are adopted to manage well operations. For each perforation block m , its well rate, $q_{\alpha,m}$, is calculated as:

$$q_{\alpha,m} = W_i \frac{\rho_\alpha K_{r\alpha}}{\mu_\alpha} (p_h - p_\alpha - \rho_\alpha g(z_h - z)), \quad (5)$$

where p_h is bottom hole pressure of a well, W_i is well index of the perforated block m , z_h is reference depth for bottom hole pressure p_h , z is depth of the perforated block m , and p_α is phase pressure of interested phase. Bottom hole pressure should be known when calculating well rate.

Various well operation strategies may be applied to a well at different time stage, such as fixed bottom hole pressure operation, fixed oil rate operation, fixed water rate operation or fixed liquid rate operation.

When the fixed bottom hole pressure operation is applied to a well, p_h is known and keeps unchanged. Since the phase pressure is known, the well rate $q_{\alpha,m}$ is known. The constraint equation for the well is

$$p_h = c, \quad (6)$$

where c is a constant set by the user input. In this case, there is no unknown to be solved for the well.

When a fixed rate operation is applied to a well, its bottom hole pressure is an unknown, and a mass conservation equation for the well should be included. For the fixed water rate operation, the constraint is

$$\sum_m q_{w,m} = q_w, \quad (7)$$

where q_w is constant. For the fixed oil rate operation, its mass conservation equation is

$$\sum_m q_{o,m} = q_o, \quad (8)$$

where q_o is constant. For the fixed liquid rate condition, the constraint equation is

$$\sum_m (q_{o,m} + q_{w,m}) = q_o + q_w. \quad (9)$$

Different constraints and combinations of them may be applied to a well at different time stages, so a scheduler should be included in a simulator, which can detect operation changes.

3 NUMERICAL METHODS

We focus on structured grids and finite difference method is applied to these models. Reservoir models are highly coupled nonlinear systems. Newton method and inexact Newton method are employed to solve the nonlinear systems. The standard Newton method solves linear system accurately while inexact Newton method solves linear system approximately. In real-world simulations, inexact Newton method can accelerate simulation and reduce running time.

3.1 Nonlinear Methods

The algorithm for inexact Newton method^[24,22] is shown by Algorithm 1.

Algorithm 1 The inexact Newton Method

- 1: Given an initial guess x^0 and stopping criterion ϵ , let $l = 0$ and assemble the right-hand side $b(x^l)$.
- 2: **while** $\|b(x^l)\| \geq \epsilon$ **do**
- 3: Assemble the Jacobian matrix A .
- 4: Find θ_l and x such that

$$\|b(x^l) - A\delta x\| \leq \theta_l \|b(x^l)\|, \quad (10)$$

- 5: Let $l = l + 1$ and $x^l = x^{l-1} + \delta x$.
 - 6: **end while**
 - 7: x^* is the solution of the nonlinear system.
-

The algorithm is the same as Newton methods except the choice of θ_l . The standard Newton method chooses a small tolerance, such as 1e-7; in this case, the solution of the corresponding linear system is accurate. The price is that the linear solver occupies large part of overall simulation time. The termination criteria of the inexact Newton method is larger compared with standard Newton method, such as 1e-2. And also, its value is set automatically. Three commonly-used choices are listed as follows^[22]:

$$\theta_l = \begin{cases} \frac{\|b(x^l) - r^{l-1}\|}{\|b(x^{l-1})\|}, \\ \frac{\|b(x^l)\| - \|r^{l-1}\|}{\|b(x^{l-1})\|}, \\ \gamma \left(\frac{\|b(x^l)\|}{\|b(x^{l-1})\|} \right)^\beta, \end{cases} \quad (11)$$

where r^l is the residual of the l -th iteration,

$$r^l = b(x^l) - J\delta x. \quad (12)$$

3.2 Preconditioner

A linear system, $Ax = b$, is derived from each Newton iteration, which is un-symmetric and ill-conditioned. Krylov solvers are employed usually. If a proper ordering technique is applied, the matrix A has the following structure,

$$A = \begin{pmatrix} A_{pp} & A_{ps} & A_{pw} \\ A_{sp} & A_{ss} & A_{sw} \\ A_{wp} & A_{ws} & A_{ww} \end{pmatrix}, \quad (13)$$

where A_{pp} is the matrix coefficients corresponding to the pressure unknowns, A_{ss} is the matrix coefficients corresponding to other unknowns, such as saturations, bubble-point pressure, and polymer concentration, and A_{ww} is the matrix coefficients corresponding to well bottom hole pressure, and other matrices are coupled ones.

A decoupling operator, which is defined as a matrix D , is applied to $Ax = b$ and it converts the original linear system to an equivalent one:

$$D^{-1}Ax = D^{-1}b. \quad (14)$$

The decoupled system is solved instead of original system. Many decoupling strategies have been proposed, such as Quasi-IMPES method^[26] and ABF method^[25]. The operators are simple and cheap to create. Here we introduce the Quasi-IMPES decoupling operator, which is defined as

$$D_{QI} = \begin{pmatrix} I & D_{ps}D_{ss}^{-1} & 0 \\ 0 & I & 0 \\ 0 & 0 & I \end{pmatrix}, \quad (15)$$

where $D_{ps} = \text{diag}(A_{ps})$ and $D_{ss} = \text{diag}(A_{ss})$.

The system is difficult to solve and many CPR-type preconditioners have been developed, such as classical CPR method and FASP method. We also designed a set of parallel CPR-type methods for black oil model and compositional model^[13]. For the sake of completeness, one of them, CPR-FPF, is introduced, where F means to apply RAS method (Restricted Additive Schwarz)^[27] to linear system $Ar = f$, and P means to apply AMG method to solve linear $A_{pp}r_p = f_p$. RAS method and AMG method are well-known to be scalable for parallel computing. The algorithm CPR-FPF method is described by Algorithm 2.

Algorithm 2 The CPR-FPF Preconditioner for preconditioning system $Ax = f$.

- 1: $x = R(A)^{-1}f$.
 - 2: $r = f - Ax$
 - 3: $x = x + \Pi_p \text{AMG}(A_{pp})^{-1} \Pi_r r$.
 - 4: $r = f - Ax$
 - 5: $x = x + R(A)^{-1}r$.
-

The RAS method is one of domain decomposition methods, which is popular for parallel computing. Each process setups a local problem, whose size is determined by local graph and overlap. Each local problem is solved by a serial solver, such as ILU(k), ILUT(p, tol) and other methods. In our simulator, the default local solver is ILU(0). There is no communication in the solution of local problem. The default overlap is one. The algebraic multigrid solver we use is BoomerAMG from HYPRE^[28].

3.3 Data structures and Algorithms

An in-house parallel platform has been developed to support the implementations of parallel reservoir simulators. The platform provides structured grid, cell-centered data, mapping, linear solvers, preconditioners, well modeling, parallel input and output, keywords parsing and visualization^[18].

Currently, regular structured hexahedral grids are provided, which have simple geometry and topology. A structured grid is shown in Fig. 1. Each cell of a grid is a hexahedron. Each cell has an integer coordinate (i, j, k) and each component $(i, j, \text{ and } k)$ is numbered along x -, y - and z -axis. Each cell also has a unique global index and when they are distributed in MPIs, each of them has a local index. Fig. 2 shows data structure of CELL, which stores geometric info, such as centroid coordinate (ctrd), face areas (area), volume (vol), index, integer coordinates in each direction and boundary type of each face.

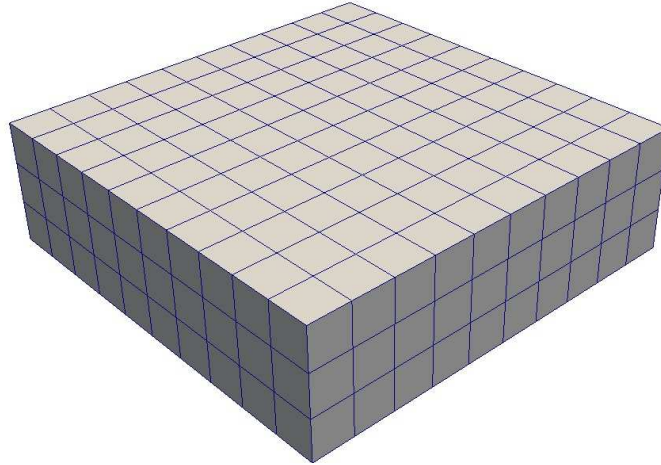


Figure 1: A structured grid

```

typedef struct CELL_
{
    COORD    ctrd;
    FLOAT    area[6];
    FLOAT    vol;

    void     *nb[6];
    INT      vert[8];
    INT      index;
    INT      idx[3];

    USHORT   bdry_type[6];
} CELL;

```

Figure 2: Data structure of CELL

A grid is distributed in N_p MPI tasks and each MPI task owns a sub-grid. Let \mathbb{G} be the grid, which has $N_g = n_x \times n_y \times n_z$ cells,

$$\mathbb{G} = \{C_1, C_2, \dots, C_{N_g}\}, \tag{16}$$

where C_i is the i -th cell of \mathbb{G} . Let \mathbb{G}_i be the sub-grid owned by the i -th MPI task. For any cell, its neighboring cells may belong to different sub-grids. When we discretize black oil models, information from

neighboring cell is required, then communication pattern can be modeled by dual graph and communication volume can be approximated by cutting edges. In our simulator, the Hilbert space-filling curve method is employed to partition a grid.

Cell-centered data module is designed to support finite difference methods and finite volume methods. The platform also provides distributed-memory matrix and vector, whose data structures are presented by Fig. 3 and 4. In Fig. 3, vector information is stored, such as number of entries belong to current process (nlocal) and number of total entries (localsize), including off-process entries. In Fig. 4, matrix distribution information, communication pattern, MPI information, and global row and column indices are stored.

```
typedef struct VEC_
{
    FLOAT    *data;
    INT      nlocal;
    INT      localsize;
} VEC;
```

Figure 3: Data structure of VEC

```
/* struct for a matrix row */
typedef struct MAT_ROW_
{
    FLOAT    *data;
    INT      *cols;
    INT      *gcols;
    INT      ncols;
} MAT_ROW;

typedef struct MAT_
{
    /* data */
    MAT_ROW  *rows;

    MAP      *map;
    COMM_INFO *cinfo;

    INT      nlocal;
    INT      localsize;
    INT      nglobal;

    int      rank;
    int      nprocs;
    MPI_Comm comm;
} MAT;
```

Figure 4: Data structure of MAT

Basic matrix-vector operations, such as

$$y = \alpha Ax + \beta y, \quad (17)$$

$$z = \alpha Ax + \beta y, \quad (18)$$

$$y = \alpha x + \beta y, \quad (19)$$

$$z = \alpha x + \beta y, \quad (20)$$

$$\alpha = \langle x, y \rangle, \quad (21)$$

$$\alpha = \langle x, x \rangle^{\frac{1}{2}}, \quad (22)$$

are implemented. With these operations, Krylov subspace solvers and preconditioners are implemented, including GMRES, BiCGSTAB, Orthomin, RAS (Restricted Additive Schwarz) preconditioner and AMG preconditioner from HYPRE^[28].

4 NUMERICAL EXPERIMENTS

The systems are used for the numerical experiments. The first one is an Blue Gene/Q from IBM. The system, Wat2Q, is located in the IBM Thomas J. Watson Research Center. Each node has 32 computer cards (64-bit PowerPC A2 processor), which has 17 cores. One of them is for the operation system and the other 16 cores for computation. The system has 32,768 CPU cores for computation. The performance of each core is really low compared with Intel processors. However, the system has strong network relative to CPU performance, and the system is scalable. The second one is GPC from SciNet. It uses Intel Xeon E5540 CPU for computation and InfiniBand for communication. Each node has two CPUs and the system has 3,864 nodes (30,912 cores). The tests focus on scalability.

4.1 Validation

This section compares our results with commercial simulators and open results to check the correctness of our implementation.

Example 1 *This example tests the Tenth SPE Comparative Solution Project, SPE10^[14], an oil-water model, which has a sufficiently fine grid. Its dimensions are $1,200 \times 2,200 \times 170$ (ft) and the fine scale cell size is $20 \times 10 \times 2$ (ft). Its grid size is $60 \times 220 \times 85$ cells (1.122×10^6 cells). This model has five wells, one of them is injection well and four are production wells. It has around 2.244 millions of unknowns. The model is highly heterogeneous, whose permeability is ranged from $6.65e-7$ Darcy to 20 Darcy, and the x -direction permeability is shown in Fig. 5^[13]. The porosity, which is demonstrated in Fig. 6^[13], ranges from 0 to 0.5. Its relative permeability of water phase is calculated as*

$$K_{rw}(s_w) = \frac{(s_w - s_{wc})^2}{(1 - s_{wc} - s_{or})^2}, \quad (23)$$

and the relative permeability of oil phase is calculated as

$$K_{ro}(s_w) = \frac{(1 - s_{or} - s_w)^2}{(1 - s_{wc} - s_{or})^2}, \quad (24)$$

where $s_{wc} = s_{or} = 0.2$. More details can be found in the reference^[14]. The solver is GMRES(30) solver. The stopping tolerance for Newton method is $1e-3$. Our results are compared with other openly available results and presented in Fig. 7 and 8.

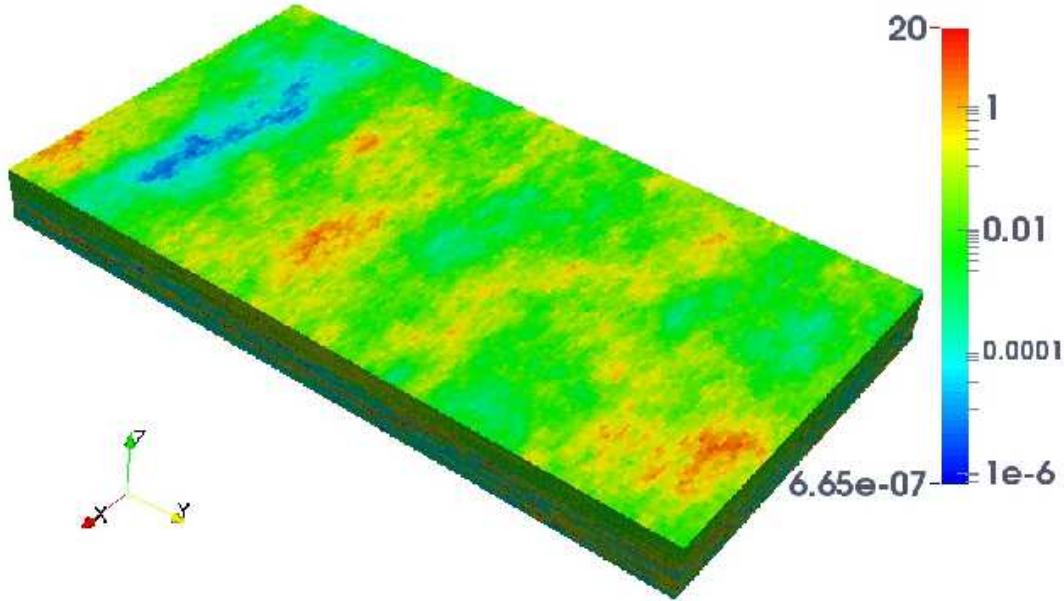


Figure 5: Permeability in X Direction of the SPE10 benchmark

Two measurements are reported, which are average pressure and oil production rate. Fig. 7 shows average pressure in each time step and it is compared with results from commercial software, from which we can see that the results match very well. Fig. 8 compares oil production rate with open results from other companies. Again, we can see these oil production results match. This example indicates our implementation is correct and our results match other simulators.

Example 2 The example test the standard black oil model and the data, mxspe009, is from CMG (Computer Modelling Group). This model is heterogeneous with permeability varying from cell to cell, porosity varying for each layer in z direction.

The grid is $24 \times 25 \times 15$ with mesh size 300ft. in x and y directions and 20, 15, 26, 15, 16, 14, 8, 8, 18, 12, 19, 18, 20, 50, 100 ft. in z direction from top to bottom. The depth of the top layer center is 9010 ft. From top to bottom the porosity varies as 0.087, 0.097, 0.111, 0.16, 0.13, 0.17, 0.17, 0.08, 0.14, 0.13, 0.12, 0.105, 0.12, 0.116, 0.157.

The initial conditions are as follows: bubble point pressure equals 3600.0 psi, reference pressure is 3600 psi at associated depth 9035 ft, depth to water-oil contact is 9950 ft, depth to gas-oil contact is 8800 ft.

All wells are vertical. There is only one injection well with maximum water injection rate 5000 bbl/day, maximum bottom hole pressure 4543.39 psi. There are 25 production wells, maximum oil rate 1500 bbl/day. More details can be found from CMG IMEX and^[30].

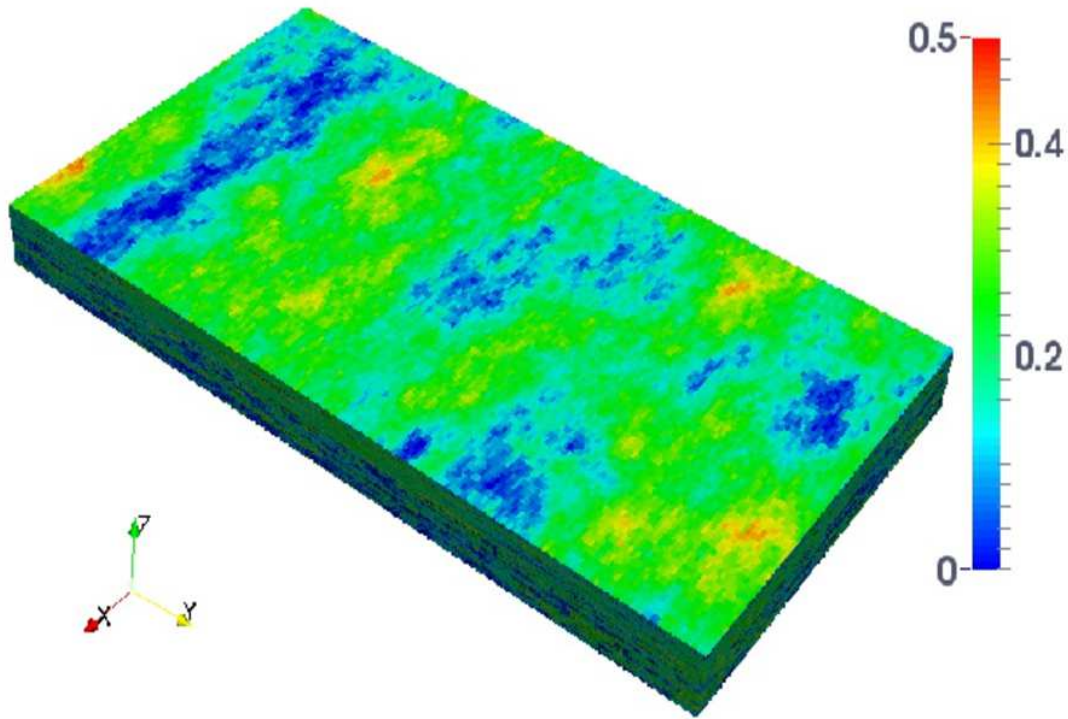


Figure 6: Porosity of the SPE10 benchmark

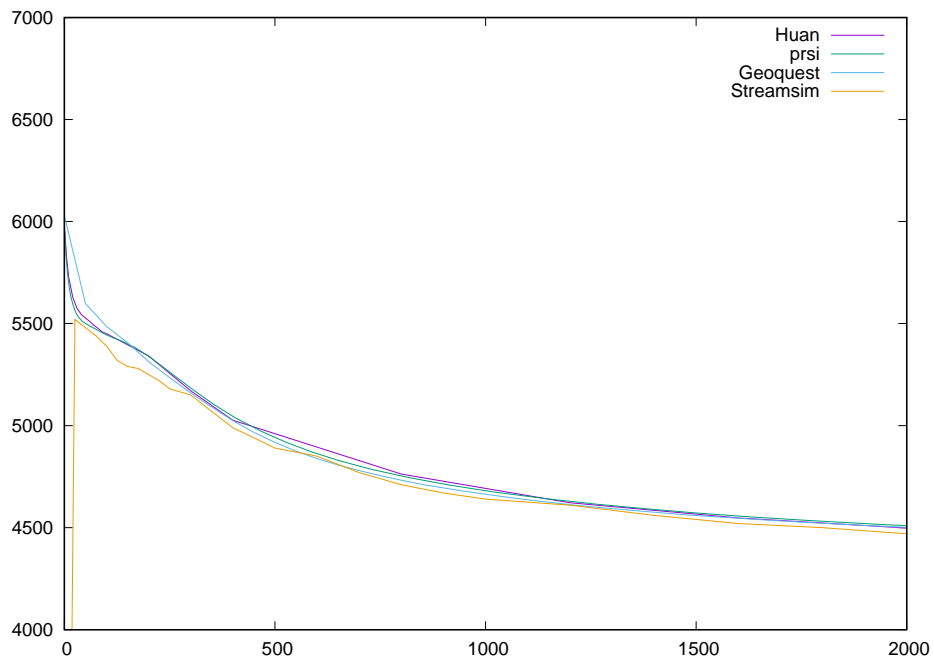


Figure 7: Average pressure of Example 1

The results from CMG IMEX are marked with "CMG IMEX" and the results from our simulator are marked with "prsi". Fig. 9 shows the oil production rates of production well 1, 2, 5 and their cumulative

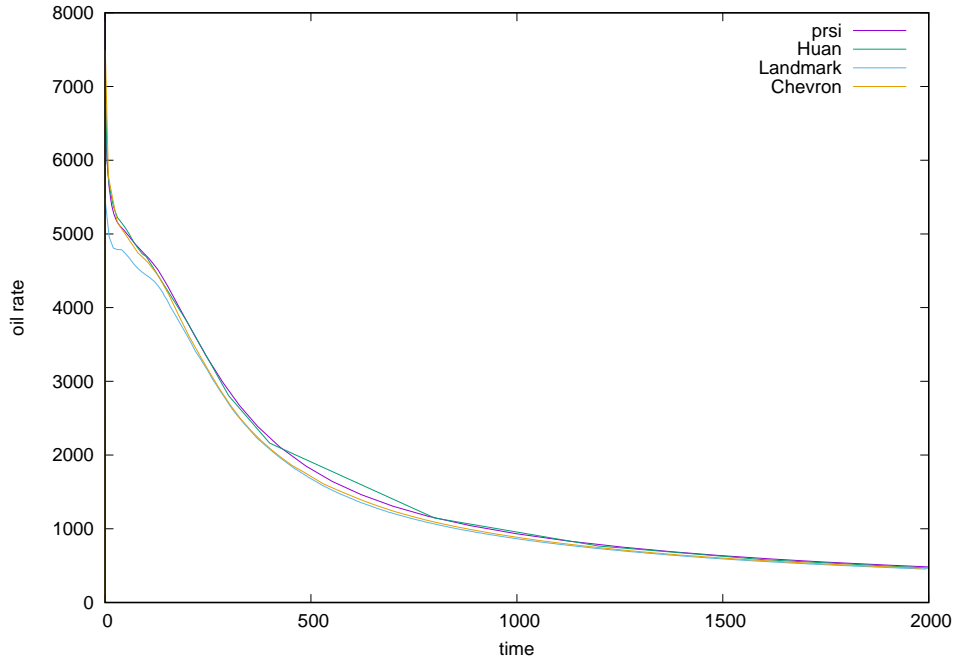


Figure 8: Oil rate of Example 1

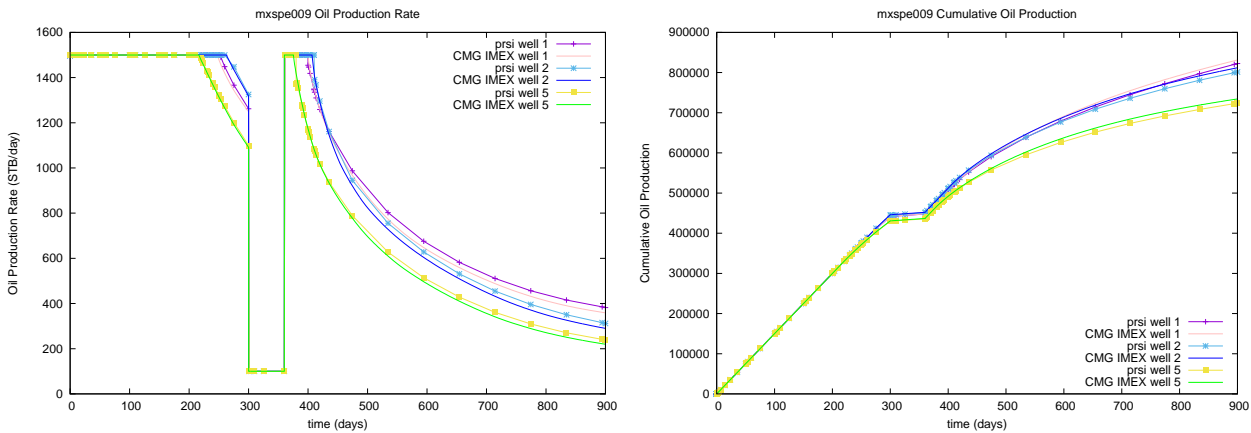


Figure 9: Oil production rate of of well 1, 2, 5 and cumulative oil production (STB) for mxspe009.

oil production. Fig. 10 shows the gas production rates and bottom-hole pressures of well 1, 2, 5. From the two figures, we can see that the results of our simulator match results from CMG IMEX.

Example 3 This is a model of two-phase oil-water problem in naturally fractured reservoir. The dual porosity dual permeability method is applied. The model, *mxfr003*, is from CMG IMEX. The grid is $10 \times 10 \times 1$ with mesh size 102.04ft. in x and y directions and 100.00ft. in z direction. The depth of the top layer center is 9010 ft.

The porosities of the matrix and the fracture are 0.1392 and 0.039585, respectively. The permeability for the matrix is 100mD in x and y directions and 10mD in z direction. The permeability for the fracture is 450md, which is 395.85mD in the original model. A new relative permeability curve for water phase is applied to fracture.

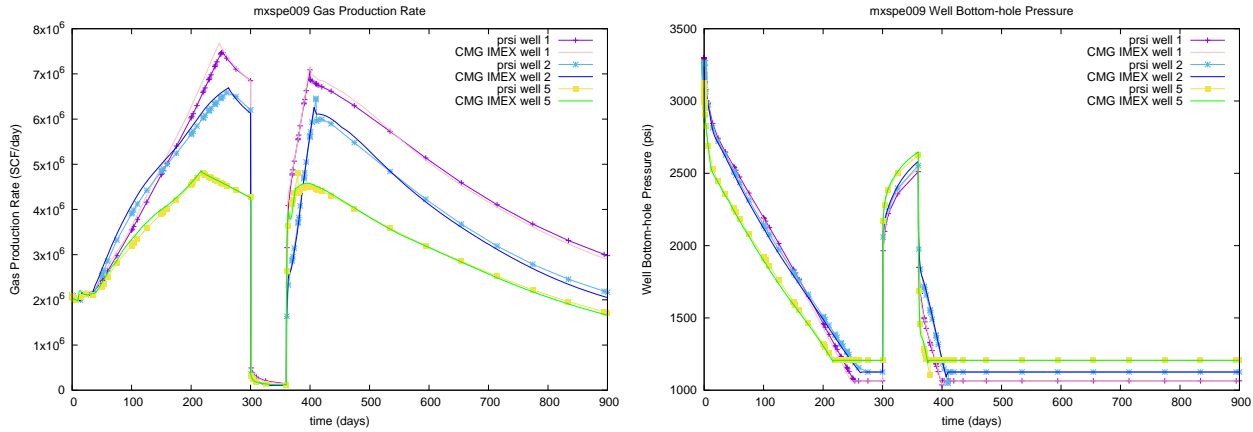


Figure 10: Gas production rate and bottom-hole pressure of well 1, 2, 5 for mxspe009.

The initial conditions are as follows: the bubble point pressure equals 15.0 psi for both matrix and fracture, the initial pressure 1479.0 psi and 1463.0 psi for matrix and fracture respectively. The oil saturation for matrix and fracture 0.92 and 0.99, respectively.

There is one injection well and one production well, both of which are vertical wells. The injection well has maximum 500 bbl/day water injection rate. The perforation is at first cell. The production well has maximum 500 bbl/day liquid production rate and minimum 15 psi bottom-hole pressure. The total simulation time is 1600 days.

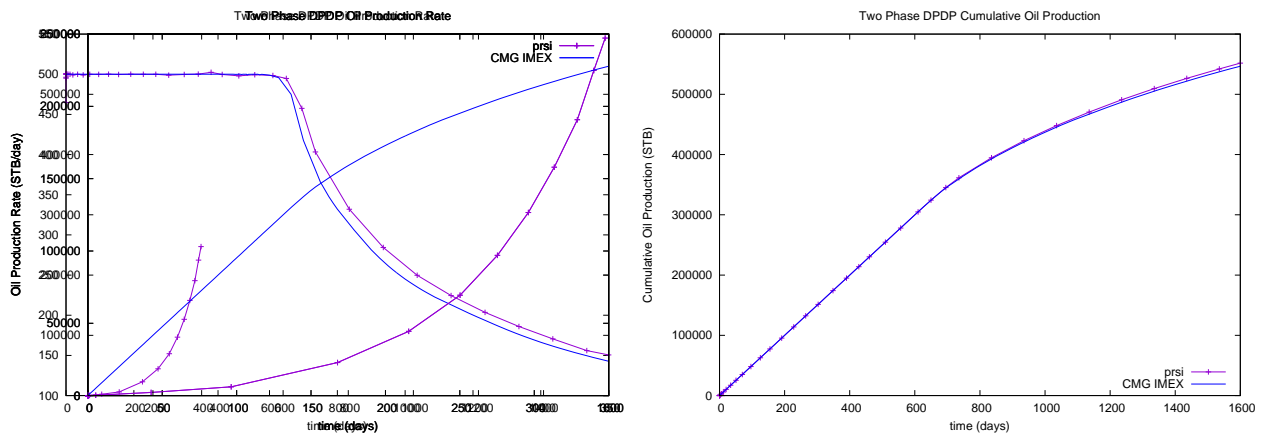


Figure 11: Oil production rate and cumulative oil production of injector and producer for mxfr003.

The oil production rates and cumulative oil production are shown in Fig. 11. Again, results from CMG IMEX are marked with "CMG IMEX" and results from our simulator are marked with "prsi". The bottom-hole pressures of injector and producer are shown in Fig. 12. Water production rate, cumulative production and water cut are shown in Fig. 13 and Fig. 14, respectively. We can see that our results match CMG IMEX's results, which indicates that our implementation is correct.

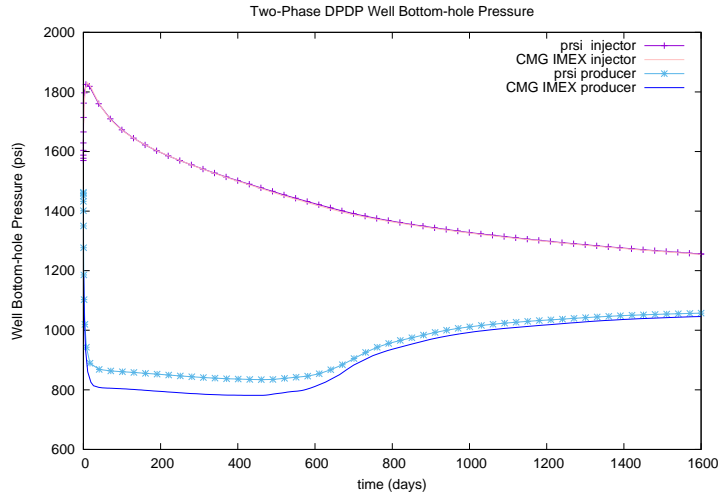


Figure 12: Bottom-hole pressure of injection and production wells for mxfr003.

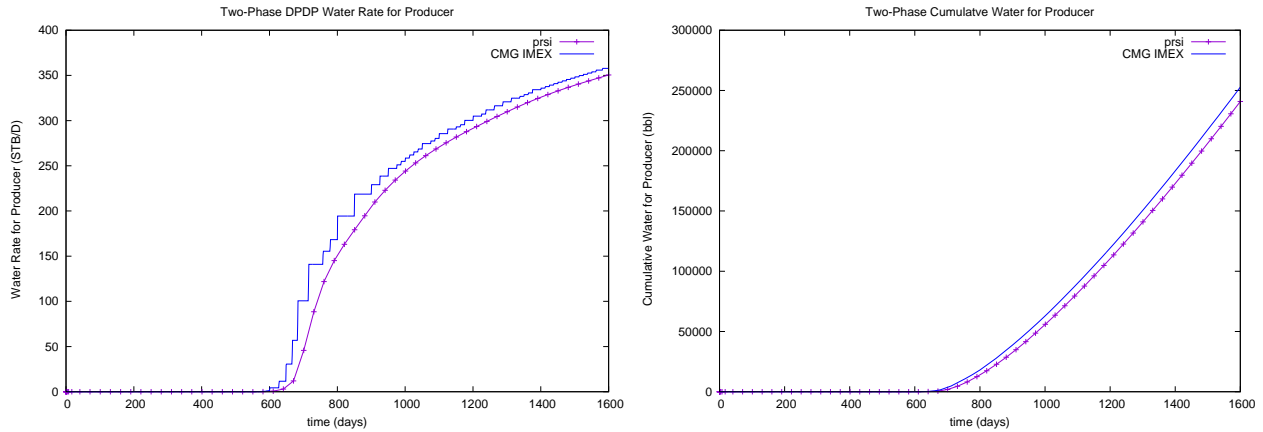


Figure 13: Water rate and cumulative production of production well for mxfr003.

4.2 Scalability

This section presents scalability results using two parallel systems.

Example 4 *The case tests two-phase oil-water model with a refined SPE10 project and each original cell is refined to 27 smaller cells. The model has around 30 millions of grid cells. The stopping criteria for inexact Newton method is $1e-2$ and maximal nonlinear iterations are 20. The linear solver is BiCGSTAB, and its maximal iterations are 100. The simulation time is 10 days. The case is run on IBM Blue Gene/Q. Numerical summaries are shown in Table 1 and scalability is presented in Fig 15.*

This case uses up to 1024 MPI processes and their speedups are compared with case that uses 128 MPI tasks. From Table 1, we can see Newton method and linear solver are robust. When more MPI tasks are employed, fewer Newton iterations are required. And each Newton iteration terminates in around 10 linear iterations. The preconditioner is effective. The running time and Fig. 15 show the parallel simulator has excellent scalability, which is almost ideal on IBM Blue Gene/Q. The results also show that our solver and preconditioner are scalable.

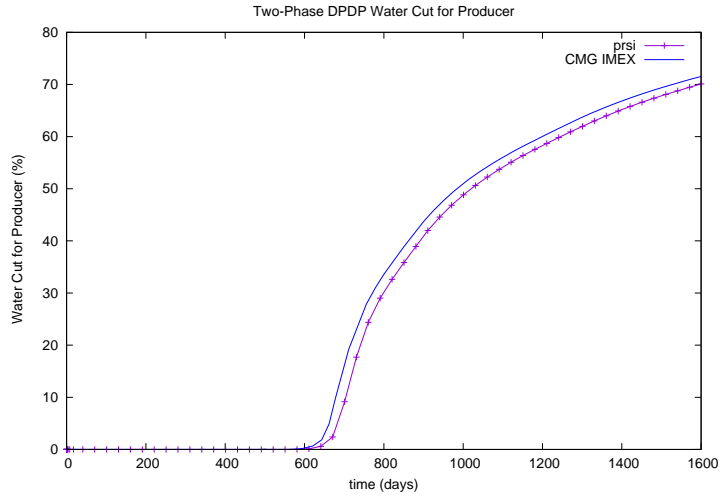


Figure 14: Water cut of production well for mxfr003.

Table 1: Numerical summaries of Example 4

# procs	# Steps	# Newton	# Solver	Time (s)
128	40	295	2470	43591.87
256	39	269	2386	20478.49
512	40	260	2664	10709.86
1024	39	259	2665	5578.75

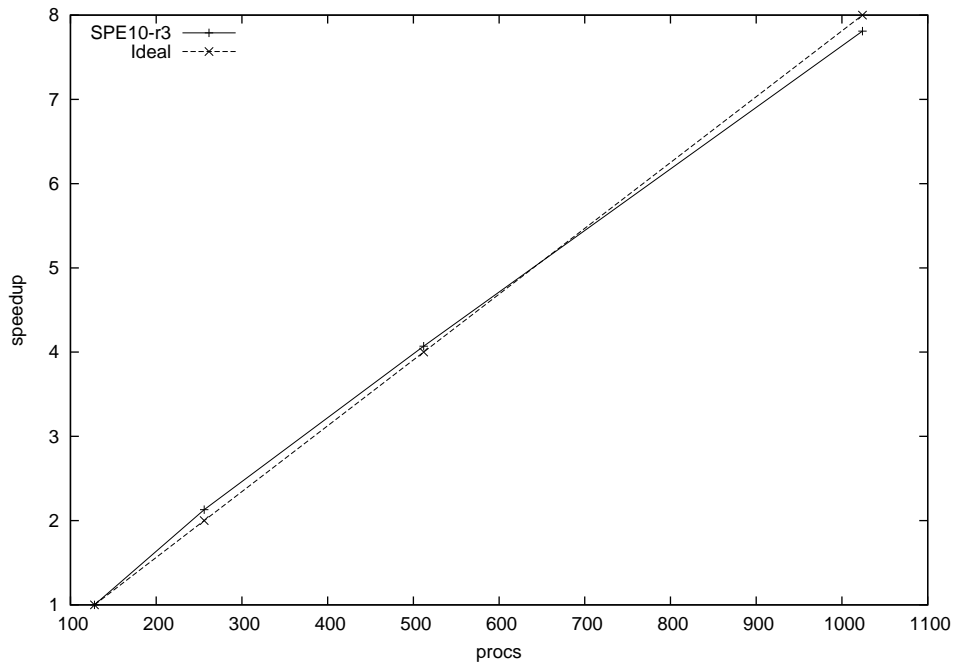


Figure 15: Scalability of Example 4

Example 5 The case also tests two-phase oil-water model, where a refined SPE10 project is used and each cell is refined to 64 smaller cells. It has around 65 millions of grid cells. The stopping criteria for inexact Newton method is $1e-2$ and its maximal nonlinear iterations are 20. The linear solver is BiCGSTAB, and its maximal iterations are 100. The simulation time is 20 days. The case is run on GPC (General Purpose Cluster). Numerical summaries are shown in Table 2 and scalability is presented in Fig. 16^[23].

Table 2: Numerical summaries of Example 5

# procs	# Steps	# Newton	# Solver	Time (s)
512	107	662	6971	26636.13
1024	108	668	7427	13772.96

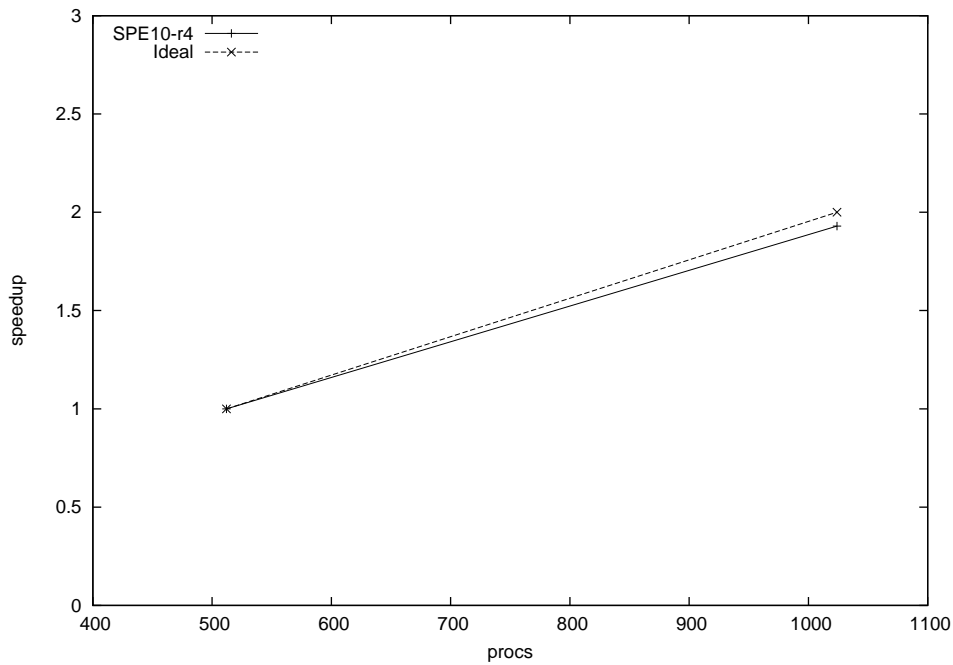


Figure 16: Scalability of Example 5

This case is larger than last example and is run on a different parallel system. Two different configurations are benchmarked. Again, Table 2 shows our nonlinear method and linear solver are robust. Each time step uses around 6.5 Newton iterations. Our linear solver and preconditioner are effective, which can solve a linear system in around 11 linear iterations. The scalability is demonstrated by Fig. 16.

Example 6 The case tests two-phase oil-water model with a refined SPE10 project and each cell is refined to 125 cells. The model has around 140 millions of cells. The stopping criteria for inexact Newton method is $1e-2$ and maximal nonlinear iterations are 20. The linear solver is BiCGSTAB, and its maximal iterations are 50. The simulation time is 10 days. The case is run on IBM Blue Gene/Q. Numerical summaries are shown in Table 3 and scalability is presented in Fig. 17.

Table 3: Numerical summaries of Example 6

# procs	# Steps	# Newton	# Solver	Time (s)
256	27	108	495	41127.23
512	27	105	515	19112.77
1024	27	102	572	9756.6
2048	26	101	625	4896.47

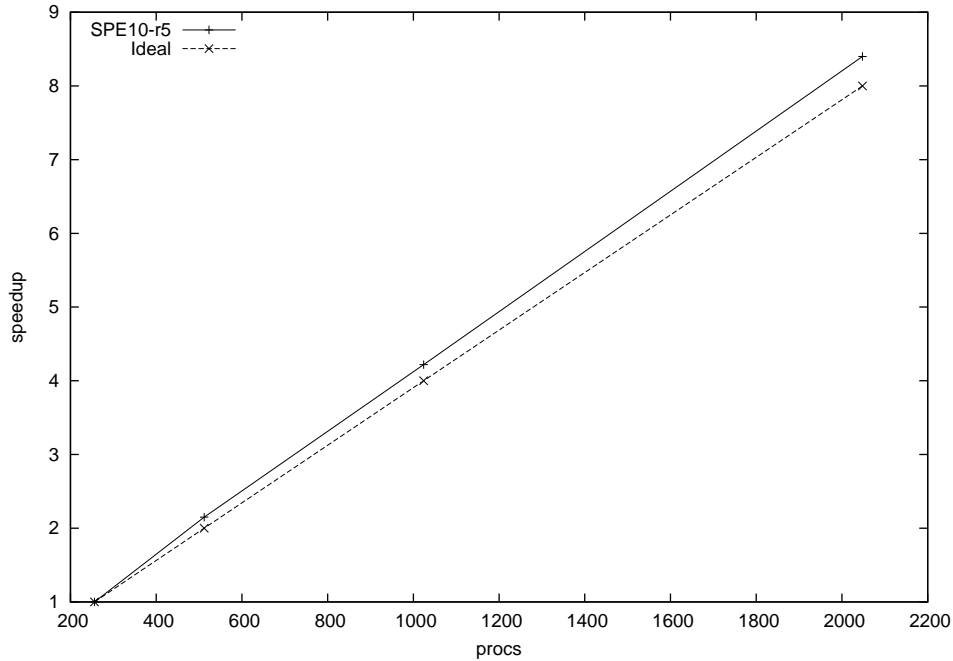


Figure 17: Scalability of Example 6

From Table 3, we can see Newton method is robust. The linear solver is also robust. However, when more MPI tasks are employed, its convergence becomes lower and lower. Average of linear iterations increases from 4.9 to 6.2. Even through, Fig. 17 show the simulator has linear scalability.

Example 7 This case tests the standard black oil model with a refined SPE10 geological model and each cell is refined to 8 cells. It has around 8.96 millions of grid cells. The stopping criteria for inexact Newton method is $1e-3$ and maximal nonlinear iterations are 15. The linear solver is BiCGSTAB, and its maximal iterations are 100. The simulation time is 200 days. The case is run on GPC (General Purpose Cluster). Numerical summaries are shown in Table 4 and scalability is presented in Fig. 18.

This example tests the standard black oil model. Table 4 shows Newton method and linear solver are robust. The running time and Fig. 18 show the simulator on GPC has a linear scalability.

Example 8 The case tests the standard black oil model using a refined SPE1 project. The model has 100 millions of cells. The stopping criteria for inexact Newton method is $1e-2$ and maximal nonlinear iterations are 15. The linear solver is BiCGSTAB, and its maximal iterations are 20. The simulation time is 10 days. The case is run on IBM Blue Gene/Q. Numerical summaries are shown in Table 5 and scalability is presented in Fig 19.

Table 4: Numerical summaries of Example 7

# procs	# Steps	# Newton	# Solver	Time (s)
64	219	1444	23597	82305.88
128	214	1402	23355	41859.71
256	218	1453	26934	22024.53
512	214	1401	24579	11548

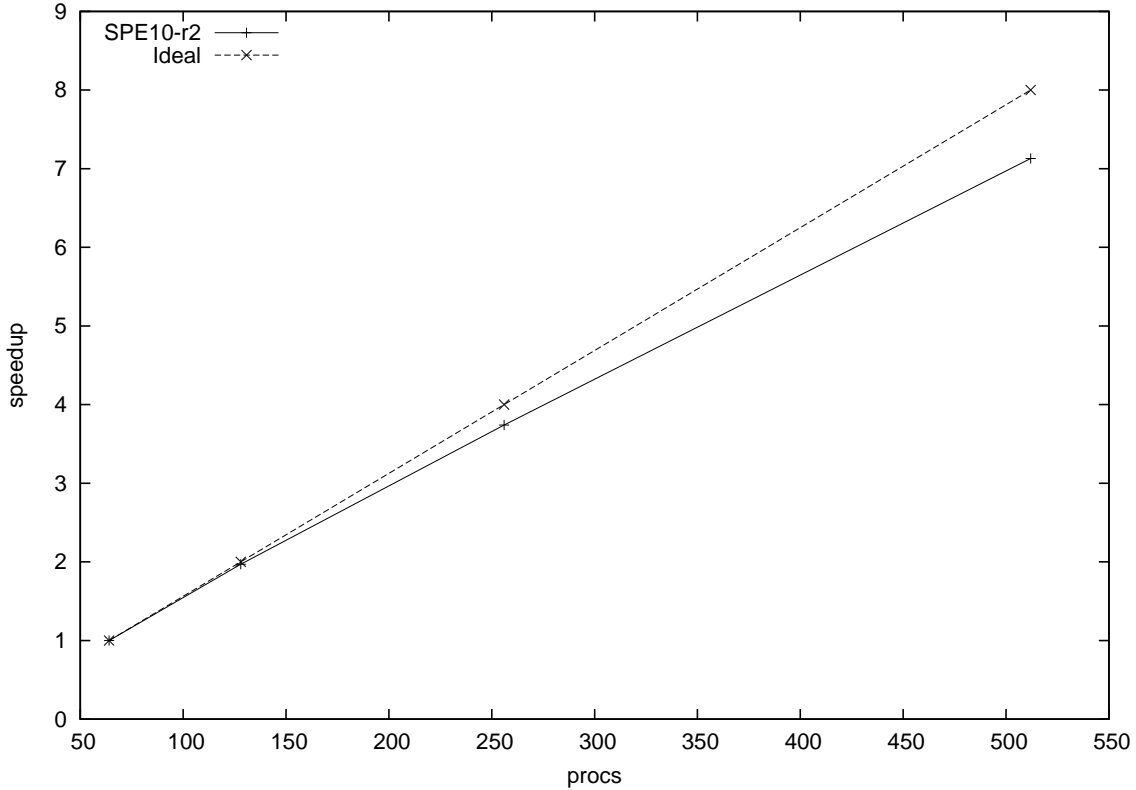


Figure 18: Scalability of Example 7

Table 5: Numerical summaries of Example 8

# procs	# Steps	# Newton	# Solver	Time (s)
512	27	140	586	11827.99
1024	27	129	377	5328.46
2048	26	122	362	2703.51
4096	27	129	394	1474.21

The case with 512 MPI tasks is the base case. From Table 5, we can see Newton method and linear solver show good convergence. Fig. 19 shows the simulator has excellent scalability and cases with 1024 MPI tasks and 2048 MPI tasks have super-linear scalability.

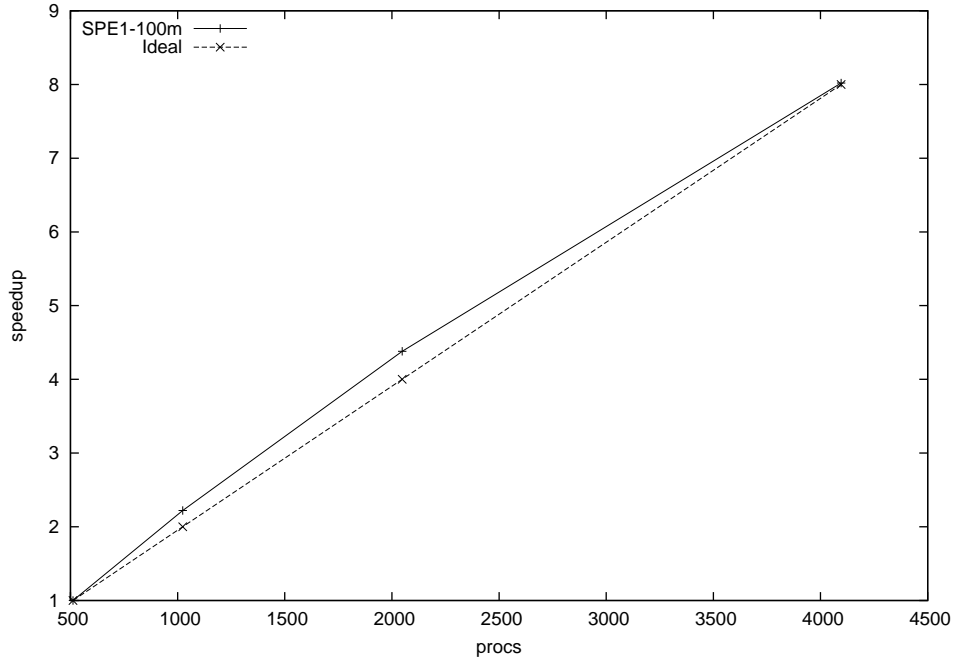


Figure 19: Scalability of Example 8

Example 9 The case tests one linear system from pressure equation and the size of the matrix is 3 billion. GMRES(30) solver is applied and it has fixed iterations of 90. The preconditioner is the RAS (Restricted Additive Schwarz) method. The case is run on IBM Blue Gene/Q. Numerical summaries are shown in Table 6 and scalability is presented in Fig 20.

Table 6: Numerical summaries of Example 9

# procs	# Solver	Time (s)
512	90	918.91
1024	90	454.04
2048	90	227.05
4096	90	116.63

This example tests the scalability of linear solver, preconditioner and SpMV. Table 6 shows that when MPI tasks are doubled, running time is cut by half. The numerical results and Fig. 20 demonstrate the simulator can model extremely large-scale reservoirs and it has excellent scalability.

5 CONCLUSION

A parallel reservoir simulator is presented, which can calculate standard black oil model and oil-water model in regular reservoirs and naturally fractured reservoirs. Their mathematical models, numerical methods and parallel implementation are introduced. Numerical experiments show that results from our

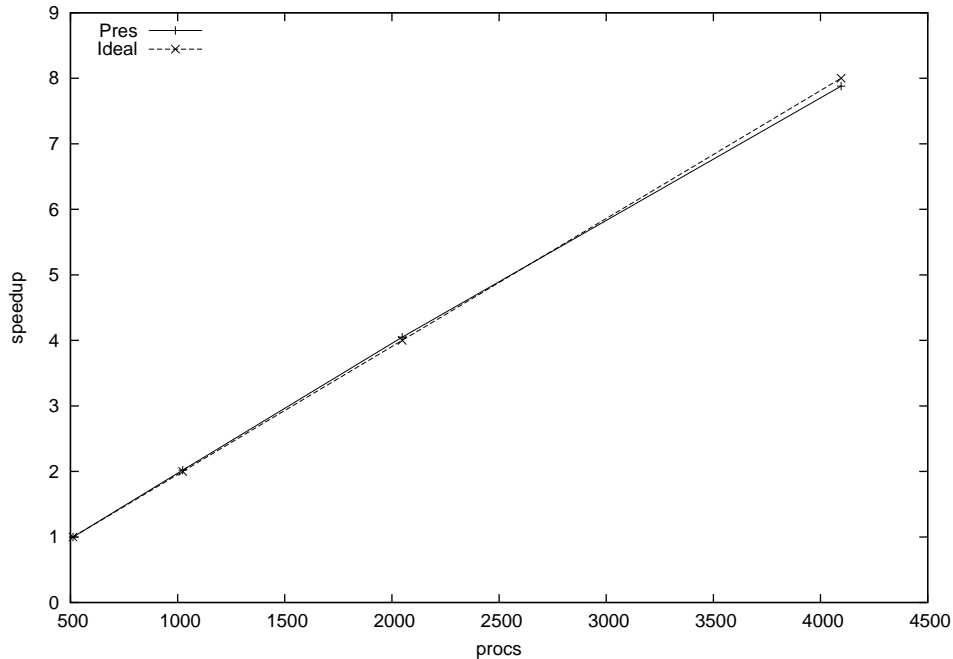


Figure 20: Scalability of Example 9

simulator match results from other simulators and our simulator has excellent scalability. The paper also demonstrates that parallel computing is a powerful tool for large-scale reservoir simulations.

ACKNOWLEDGEMENTS

The support of Department of Chemical and Petroleum Engineering, University of Calgary and Reservoir Simulation Research Group is gratefully acknowledged. The research is partly supported by NSERC, AIEES, Foundation CMG, AITF iCore, IBM Thomas J. Watson Research Center, the Frank and Sarah Meyer FCMG Collaboration Centre for Visualization and Simulation, WestGrid (www.westgrid.ca), SciNet (www.scinethpc.ca) and Compute Canada (www.computeCanada.ca).

References

- [1] J. Rutledge, D. Jones, W. Chen, and E. Chung, The Use of Massively Parallel SIMD Computer for Reservoir Simulation, SPE Computer Applications, 1991, 04, 16.
- [2] G. Shiralkar, R. Stephenson, W. Joubert, O. Lubeck, and B. van Bloemen Waanders, A production quality distributed memory reservoir simulator, SPE Reservoir Evaluation & Engineering, 1998, 1, 400.
- [3] T. Kaarstad, J. Froyen, P. Bjorstad, and M. Espedal, A Massively Parallel Reservoir Simulator, Symposium on Reservoir Simulation, Society of Petroleum Engineers, San Antonio, 12-15 February 1995.

- [4] J. Killough, D. Camilleri, B. Darlow, and J. Foster, Parallel Reservoir Simulator Based on Local Grid Refinement, SPE-37978, SPE Reservoir Simulation Symposium, Dallas, 1997.
- [5] A. Dogru, L. Fung, U. Middy, T. Al-Shaalan, and J. Pita, A next-generation parallel reservoir simulator for giant reservoirs, SPE/EAGE Reservoir Characterization & Simulation Conference. 2009.
- [6] L. Zhang, A Parallel Algorithm for Adaptive Local Refinement of Tetrahedral Meshes Using Bisection, Numer. Math.: Theory, Methods and Applications, 2009, 2, 65–89.
- [7] L. Zhang, T. Cui, and H. Liu, A set of symmetric quadrature rules on triangles and tetrahedra, J. Comput. Math, 2009, 27(1), 89–96.
- [8] J. Wallis, R. Kendall, and T. Little, Constrained residual acceleration of conjugate residual methods, SPE Reservoir Simulation Symposium, 1985.
- [9] H. Cao, T. Schlumberger, A. Hamdi, J. Wallis, and H. Yardumian, Parallel scalable unstructured CPR-type linear solver for reservoir simulation. SPE Annual Technical Conference and Exhibition. 2005.
- [10] T. Al-Shaalan, H. Klie, A. Dogru, and M. Wheeler, Studies of Robust Two Stage Preconditioners for the Solution of Fully Implicit Multiphase Flow Problems. SPE Reservoir Simulation Symposium. 2009.
- [11] X. Hu, W. Liu, G. Qin, J. Xu, and Z. Zhang, Development of a fast auxiliary subspace pre-conditioner for numerical reservoir simulators, SPE Reservoir Characterisation and Simulation Conference and Exhibition. 2011.
- [12] Z. Chen, G. Huan, and Y. Ma, Computational methods for multiphase flows in porous media, Vol. 2. Siam, 2006.
- [13] H. Liu, K. Wang, and Z. Chen, A family of constrained pressure residual preconditioners for parallel reservoir simulations, Numerical Linear Algebra with Applications, Vol. 23(1), 2016, 120-146.
- [14] M. Christie, and M. Blunt, Tenth SPE comparative solution project: A comparison of upscaling techniques. SPE Reservoir Evaluation & Engineering 4.4 (2001): 308-317.
- [15] B. Wang, S. Wu, Q. Li, X. Li, H. Li, C. Zhang, and J. Xu, A Multilevel Preconditioner and Its Shared Memory Implementation for New Generation Reservoir Simulator, SPE-172988-MS, SPE Large Scale Computing and Big Data Challenges in Reservoir Simulation Conference and Exhibition, 15-17 September, Istanbul, Turkey, 2014.
- [16] K. Wang, L. Zhang, and Z. Chen, Development of Discontinuous Galerkin Methods and a Parallel Simulator for Reservoir Simulation, SPE-176168-MS, SPE/IATMI Asia Pacific Oil & Gas Conference and Exhibition, 20-22 October, Nusa Dua, Bali, Indonesia, 2015.
- [17] D. Peaceman, Interpretation of Well-Block Pressures in Numerical Reservoir Simulation, SPE-6893, 52nd Annual Fall Technical Conference and Exhibition, Denver, 1977.

- [18] H. Liu, K. Wang, Z. Chen, K. Jordan, J. Luo, and H. Deng, A Parallel Framework for Reservoir Simulators on Distributed-memory Supercomputers, SPE-176045-MS, SPE/IATMI Asia Pacific Oil & Gas Conference and Exhibition, Nusa Dua, Indonesia, 20 C 22 October, 2015.
- [19] W. Guan, C. Qiao, H. Zhang, C. Zhang, M. Zhi, Z. Zhu, Z. Zheng, W. Ye, Y. Zhang, X. Hu, Z. Li, C. Feng, Y. Xu, and J. Xu, On Robust and Efficient Parallel Reservoir Simulation on Tianhe-2, SPE-175602-MS, SPE Reservoir Characterisation and Simulation Conference and Exhibition, 14-16 September, Abu Dhabi, UAE, 2015.
- [20] M. Wheeler, Advanced Techniques and Algorithms for Reservoir Simulation, II: The Multiblock Approach in the Integrated Parallel Accurate Reservoir Simulator (IPARS), The IMA Volumes in Mathematics and its Applications, Springer New York, pp: 9-19, 2002.
- [21] K. Wang, H. Liu, and Z. Chen, A scalable parallel black oil simulator on distributed memory parallel computers, Journal of Computational Physics, Vol 301, 19-34.
- [22] T. Chen, N. Gewecke, Z. Li, A. Rubiano, R. Shuttleworth, and B. Yang, X. Zhong, Fast Computational Methods for Reservoir Flow Models, 2009.
- [23] H. Liu, K. Wang, Z. Chen, B. Yang and R. He, Large-scale Reservoir Simulations on Distributed-memory Parallel Computers, SpringSim-HPC 2016 April 3-6 Pasadena, CA, USA.
- [24] W. Gander, G. Golub, and R. Strebler, Least Squares Fitting of Circles and Ellipses, BIT Numerical Mathematics, 1994; 34(4): 558-578.
- [25] R. Bank, T. Chan, W. Coughran Jr., and R. Smith, The Alternate-Block-Factorization procedure for systems of partial differential equations, BIT Numerical Mathematics, 1989; 29(4): 938-954.
- [26] S. Lacroix, Y. Vassilevski, and M. Wheeler, Decoupling preconditioners in the implicit parallel accurate reservoir simulator (IPARS), Numerical linear algebra with applications, 2001; 8(8): 537-549.
- [27] X. Cai and M. Sarkis, A restricted additive Schwarz preconditioner for general sparse linear systems, SIAM Journal on Scientific Computing, 1999; 21(2): 792-797.
- [28] R. D. Falgout, and U.M. Yang, HYPRE: A library of high performance preconditioners, Lecture Notes in Computer Science, Springer Berlin Heidelberg, 2002. 632-641.
- [29] K. Wang, H. Liu, J. Luo, and Z. Chen, Parallel Simulation of Full-Field Polymer Flooding, The 2nd IEEE International Conference on High Performance and Smart Computing, 2016.
- [30] J.E. Killough, Ninth SPE Comparative Solution Project: A Reexamination of Black-Oil Simulation, SPE-29110-MS, SPE Reservoir Simulation Symposium, 12-15 February, San Antonio, Texas, 1995.